Identification and characterization of developmental genes in streptomyces

Zhang, L.

II

SepG acts as a membrane anchor for SsgB to allow recruitment of FtsZ to division sites in *Streptomyces coelicolor*

Le Zhang, Joost Willemse, Dennis Claessen and Gilles P. van Wezel

Submitted for publication

ABSTRACT

In bacteria that divide by binary fission, a single septum is formed at midcell. Landmark events are the localization of the cell-division scaffold protein FtsZ, and the timely segregation of the nucleoids. Here we show that SepG acts as membrane anchor for SsgB, which is a determining step for the recruitment of FtsZ in *Streptomyces*. FRET imaging revealed direct interaction between SepG and SsgB. Without SepG, SsgB briefly localizes in foci but then rapidly disperses along the membrane, consistent with SepG anchoring the SsgB-FtsZ complex. While SsgB remains associated with FtsZ, SepG re-localizes to sites of active spore-wall synthesis. Expanded doughnut-shaped nucleoids are formed in *sepG* null mutants, suggesting that SepG acts to prevent DNA damage during spore-wall synthesis. Thus, our data provide the first insights into the function of *sepG*, which is one of the last genes in the *dcw* cluster of Gram-positive bacteria whose function was still unresolved.

INTRODUCTION

Most unicellular bacteria grow and divide by binary fission, which involves an increase in cell length, chromosome replication and segregation and septum formation, eventually resulting in two daughter cells that each inherits a single copy of the chromosome. Chromosome organization and segregation are tightly coordinated with the spatial and temporal initiation of cell division. The prokaryotic cell division scaffold is formed by the tubulin homolog FtsZ (Bi and Lutkenhaus, 1991), which forms a contractile ring (or Z ring) that mediates recruitment of the cell division machinery to the mid-cell position (reviewed (Goehring and Beckwith, 2005; Adams and Errington, 2009)). In unicellular bacteria, septum-site localization and Z-ring stabilization is mediated by a number of proteins including FtsA and ZipA (Hale and de Boer, 1997; RayChaudhuri, 1999; Pichoff and Lutkenhaus, 2002), ZapA (Gueiros-Filho and Losick, 2002) and SepF (Hamoen *et al.*, 2006; Ishikawa *et al.*, 2006). The process of Z-ring (dis-)assembly during division is actively controlled (reviewed in (Romberg and Levin, 2003)).

Streptomycetes are filamentous Gram-positive soil bacteria that have a complex multicellular life cycle (Claessen *et al.*, 2014; Flärdh and Buttner, 2009) and produce over 60% of all known antibiotics and many other bioactive natural products (Hopwood, 2007). Expression of these natural products is typically coordinated with the onset of spore development (van Wezel and McDowall, 2011). The vegetative mycelium consists of syncytial cells separated by widely spaced crosswalls (Wildermuth and Hopwood, 1970). During sporulation-specific cell division, FtsZ initially assembles in long filaments in the aerial hyphae, then as regular foci, to finally form a ladder of Z rings (Schwedock *et al.*, 1997). Eventually, cytokinesis results in long chains of spores, following a complex process of coordinated cell division and DNA segregation (Jakimowicz and van Wezel, 2012; McCormick and Losick, 1996)). Cell division is not essential for growth of *Streptomyces*, which provides a unique system for the study of this process (McCormick *et al.*, 1994; McCormick and Losick, 1996).

The mycelial life style of streptomycetes imposes specific requirements for cell division control, in particular due to the lack of a defined midcell position and the synchronous formation of multiple septa. The canonical model for the control of Z-ring formation involves the action of negative control systems such as Min, which prevents Z-ring assembly at the cell poles (Marston *et al.*, 1998; Raskin and de Boer, 1997), and nucleoid occlusion that prevents formation of the Z ring over non-segregated chromosomes (Bernhardt and

de Boer, 2005; Woldringh *et al.*, 1991; Wu and Errington, 2004; Wu and Errington, 2012). However, in *Streptomyces* septum-site localization is positively controlled, via the recruitment of FtsZ by SsgB, which in turn depends on the action of SsgA (Willemse *et al.*, 2011). The SsgA-like proteins (SALPs) are proteins that uniquely occur in actinomycetes (Girard *et al.*, 2013). This different mode of division control most likely explains the absence of direct homologs of Min and Noc proteins and of the canonical Z-ring anchoring proteins. SepF and DivIVA are rare examples of cell division control proteins shared between *Streptomyces* and other bacteria, and of these, DivIVA is not involved in the control of division, but is instead required for driving apical (tip) extension and growth (Flärdh, 2003a). The concept of positive control of cell division is more widespread in bacteria, as it was also found in *Myxococcus xanthus* where the ParA-like protein PomZ recruits FtsZ (Treuner-Lange *et al.*, 2013), while the recent discovery that *Bacillus* cells divide at midcell in the absence of Min and Noc may be explained by a positive control-like mechanism, although there the mechanism of septum positioning is unknown (Rodrigues and Harry, 2012).

With the recruitment of FtsZ by SsgB, another important question is left unaddressed, namely how the highly symmetrical spacing between the sporulation septa is achieved; in other words, how is the localization of SsgB itself orchestrated? We previously suggested that the regularly spaced nucleoids might provide the boundaries for Z-ring assembly, in analogy with a nucleoid-occlusion mechanism (Willemse *et al.*, 2011). One possible candidate is the conserved *ylmG* gene, which lies between *sepF* and *divIVA* in the *dcw* cluster (division and cell-wall synthesis), in particular in actinobacteria, firmicutes and cyanobacteria, as well as in chloroplasts of photosynthetic eukaryotes. The YlmG ortholog AtYLMG1-1 of the plant *Arabidopsis thaliana* is a membrane protein that controls nucleoid morphology (Kabeya *et al.*, 2010). Knock-down of the gene via expression of an anti-sense RNA impaired nucleoid partitioning and changed the morphology of nucleoids in *A. thaliana*. Similar results were obtained in the cyanobacterium *Synechococcus elongates* (Kabeya *et al.*, 2010). However, deletion of *ylmG* in *Streptococcus* did not result in any noticeable defects in cell division or nucleoid segregation (Marbouty *et al.*, 2009).

In this work, we show that after the initial localization of SsgB by SsgA at a central location in the hyphae, YlmG is required for the subsequent membrane anchoring of SsgB and consequentially also for the recruitment of FtsZ. The protein was therefore renamed SepG. The SepG protein localizes to the periphery of the future spore compartments, where it contributes to main-

tenance of chromosome compaction. In the absence of SepG, the nucleoid expands to the outer limits of the spore compartments, compromising septum synthesis. Taken together, our data provide the first insights into the function of SepG that is well conserved in Gram-positive bacteria, and show that SepG is required for positive control of cell division as well as for nucleoid morphogenesis in *Streptomyces*.

MATERIALS AND METHODS

Bacterial strains and media

The bacterial strains used in this work are listed in Table 1. *E. coli* strains JM109 (Sambrook *et al.*, 1989) and ET12567 (MacNeil *et al.*, 1992) were used for routine cloning and for isolation of non-methylated DNA, respectively. *E. coli* transformants were selected on LB agar media containing the relevant antibiotics and grown O/N at 37°C. *Streptomyces coelicolor* A3(2) M145 was used as parental strain to construct mutants. All media and routine *Streptomyces* techniques are described in the *Streptomyces* manual (Kieser *et al.*, 2000). Yeast extract-malt extract (YEME) and tryptone soy broth with 10% sucrose (TSBS) were the liquid media for standard cultivation. Regeneration agar with yeast extract (R2YE) was used for regeneration of protoplasts and with appropriate antibiotics for selection of recombinants (Kieser *et al.*, 2000). Soy flour mannitol (SFM) agar plates were used to grow *Streptomyces* strains for preparing spore suspensions and for morphological characterization and microscopy.

Table 1. Bacterial strains.

Bacterial strains	Genotype	Reference
E. coli JM109	See reference	(Sambrook *et al.*, 1989)
E. coli ET12567	See reference	(MacNeil *et al.*, 1992)
M145	*S. coelicolor* A3(2) SCP1- SCP2-	(Kieser *et al.*, 2000)
K202	M145 + KF41	(Grantcharova *et al.*, 2005)
JSC2	FM145 + genomic ssgB-egfp fusion + pGWS523	(Willemse *et al.*, 2011)
JSC3	FM145 + genomic SsgB-mCherry fusion + pKF41	(Willemse *et al.*, 2011)
GAL1	M145Δ*ylmG*	This work
GAL2	M145 + pGWS755	This work
GAL3	GAL1 + KF41	This work
GAL4	GAL1 + pGWS116	This work
GAL5	GAL1 + pGWS526	This work
GAL7	GAL1 + pGWS755	This work
GSA3	M145Δ*ssgA*(::*aadA*)	(van Wezel *et al.*, 2000b)
GSB1	M145Δ*ssgB*(::*aac(3)IV*)	(Keijser *et al.*, 2003)
GAL93	GAL1 + pGWS771	This work
GAL94	M145 + pGWS791 + pGWS116	This work
GAL95	M145 + pGWS791 + pGWS526	This work
GAL96	M145 + pGWS755 + pGWS529	This work

Plasmids and constructs

All plasmids and constructs described in this work are summarized in Table 2 and oligonucleotides are listed in Table 3. PCRs were carried out with Phusion enzyme (Finnzymes, Bioké, Leiden, the Netherlands) as previously described (Colson *et al.*, 2007).

Table 2. Plasmids and constructs.

Plasmid and constructs	Description	Reference
pWHM3	*E. coli*/*Streptomyces* shuttle vector, around 100 copies per chromosome in both *E. coli* and *Streptomyces*.	(Vara *et al.*, 1989)
pGWS725	pWHM3 with deleted XbaI site from multiple cloning sites region.	This work
pSET152	*E. coli*/*Streptomyces* shuttle vector, around 100 copies per chromosome in *E. coli* and integrative in the φC31 attachment site in *Streptomyces*	(Bierman *et al.*, 1992)
pGWS523	FtsZ-mCherry from its native promoter in pSET152-derivative vector, containing the neomycin resistance cassette	(Willemse et al., 2011)
pHJL401	*E. coli*/*Streptomyces* shuttle vector, around five per chromosome copies in *Streptomyces* and around 100 copies per chromosome in *E. coli*	(Larson and Hershberger, 1986)
pGWS731	pWHM3 containing flanking regions of *S. coelicolor* SCO2078 with apra-*loxP* inserted in between	This work
pUWL-Cre	Plasmid expressing Cre-recombinase	(Fedoryshyn *et al.*, 2008)
pKF41	integrative construct expressing *ftsZ-egfp* from the natural *ftsZ* promoter region	(Grantcharova *et al.*, 2005)
pGWS755	pSET152 harboring the *ylmG-egfp* under the control of the *ftsZ* promoter of *S. coelicolor*	This work
pGWS771	pSET152 harboring the +1/+294 region of *ylmG* under the control of the *ftsZ* promoter of *S. coelicolor*	This work
pGWS116	pHJL401 expressing SsgA-eGFP	(Noens *et al.*, 2007)
pGWS526	pHJL401 expressing SsgB-eGFP	(Willemse *et al.*, 2011)
pGWS791	pSET152 with *ylmG-mCherry* under the control of the *ftsZ* promoter of *S. coelicolor*	This work
pGWS529	pHJL401 expressing FtsZ-mCherry from its native promoter	This work

The strategy for creating knock-out mutants is based on the unstable multi-copy vector pWHM3 (Vara et al., 1989), essentially as described previously (Świątek *et al.*, 2012). The -1442/+6 and +277/+1521 regions relative to the translational start of *ylmG* (SCO2078) were amplified by PCR from the *S. coelicolor* M145 genome using primer pairs ylmG_LF_1442 and ylmG_LR+6 and ylmG_RF+277 and ylmG_RR+1521, respectively (Table 3). Fragments were then cloned into EcoRI/BamHI-digested pGWS725, with the oligonucleotides designed such as to create a unique XbaI site in-between the flanking regions. The apramycin resistance cassette *aac(3)IV* flanked by *loxP* sites was then cloned via the engineered XbaI site to generate knock-out construct pGWS731. The presence of *loxP* sites allows the efficient removal of the apramycin resistance cassette from the chromosome following the introduction of plasmid pUWL-Cre that expresses the Cre recombinase (Fedoryshyn *et al.*, 2008). For complementation of the *ylmG* null mutant the integrative vector pSET152 harboring the coding sequence (+1/+294 region) of *ylmG* under control of the *ftsZ* promoter (pGWS771) was used.

To obtain a construct expressing YlmG-eGFP, we used plasmid pKF41 which expresses FtsZ-eGFP from the native *ftsZ* promoter region (Grantcharova et al., 2005). The insert was excised using restriction enzymes BglII and NotI, cloned into the integrative vector pSET152. To replace the *ftsZ* coding region by that of *ylmG*, the construct was digested with StuI and BamHI, and the *ylmG* gene was PCR-amplified from the genome of *S. coelicolor* using primer pair ylmG_F+1 and ylmG_R+282. The PCR product was subsequently cloned as a StuI-BamHI fragment in between *ftsZ*p and *egfp* to generate pGWS755. To generate a similar construct expressing YlmG-mCherry, the *egfp* gene in pGWS755 was removed by digestion with BamHI and NotI and replaced by *mCherry* to generate pGWS791.

Table 3. Oligonucleotides.

Name	**5'-3' sequence** [#]
ylmG_LF-1442	GTCA**GAATTC**GCGGACGATGTGCGCATTCTCTCG
ylmG_LR+6	GTCAGAAGTTATCCATCACC**TCTAGA**GCTCATGACCTGTGCTTCCCTCTC
ylmG_RF+277	GTCAGAAGTTATCGCGCATC**TCTAGA**CAGCTGTGAGCGATGAGAGAGATAC
ylmG_RR+1521	GTCA**GGATCC**TCGATCAGGAACCCGCGCATCGGC
ylmG_F+1	GTCAGAATTC**AGGCCT**TCGACATGAGCGTGGTCCTGGATGTC
ylmG_R+282	GTCAAAGCTT**GGATCC**AGCTGGCTCACGATCGAGAT
ylmG_R+294	GCTA**GGATCC**TCTCATCGCTCACAGCTGGCT

[#] Restriction sites used for cloning are underlined and in bold face. GGATCC, BamHI; GAATTC, EcoRI; AGGCCT stuI; TCTAGA, XbaI.

Microscopy

Sterile cover slips were inserted at an angle of 45 degrees into SFM agar plates, and spores of *S. coelicolor* and derivatives were carefully inoculated at the intersection angle. After incubation at 30°C for 3 to 5 days, cover slips were positioned on a microscope slide prewetted with 5 µl of 1x PBS. Fluorescence and corresponding light micrographs were obtained with a Zeiss Axioscope A1 upright fluorescence microscope (with an Axiocam Mrc5 camera at a resolution of 37.5 nm/pixel). The green fluorescent images were created using 470/40 nm band pass excitation and 525/50 band pass detection, while for the red channel 550/25 nm band pass excitation and 625/70 nm band pass detection was used (Willemse and van Wezel, 2009). DAPI was detected using 370/40 nm excitation with 445/50 nm emission band filter. For membrane staining FM5-95 was used and for DNA staining DAPI (all obtained from Molecular Probes). To obtain a sufficiently dark background, all images were corrected by setting the signal outside the hyphae to zero. These corrections were made using Adobe Photoshop CS4.

Chromosome distribution in spores of *S. coelicolor* strains was studied using stimulated emission depletion (STED) microscopy. For this, patches of the different *Streptomyces* strains were grown on SFM agar plates and incubated at 30°C for 5 days. Live cells were stained with Syto 9 (0.5 mM) for 5 minutes, after which STED was performed with a Leica TCS STED CW system with 488 nm excitation (5% laser power) and depletion at 592 nm (30% laser power).

Morphological studies on surface grown aerial hyphae and/or spores by cryo-scanning electron microscopy were performed using a JEOL JSM6700F scanning electron microscope as described previously (Colson et al., 2008). Transmission electron microscopy (TEM) for the analysis of cross-sections of hyphae and spores was performed with a FEI Tecnai 12 BioTwin transmission electron microscope as described (Noens et al., 2005).

Acceptor photobleaching was performed with a Zeiss Imager. eGFP was excited with a 488 nm laser (5% intensity) and emission was detected from 505-530 nm. mCherry was excited with 543nm laser (5% intensity) and detected with a 560 long-pass. Both channels were recorded sequentially to prevent signal cross-bleeding. Bleaching was performed with the 543 nm laser at maximum intensity for 25 iterations. For all experiments, the original intensity was determined as the average of three pre-bleach frames and the post bleaching intensity was set as the average of the first three post-bleach frames. For SsgA-eGFP with YlmG-mCherry (no interaction) eleven independent experiments were carried out, for the combination of FtsZ-mCherry and

YlmG-eGFP eighteen and for SsgB-eGFP and YlmG-mCherry twenty four. The average post-bleach intensity was calculated relative to the pre-bleach intensity, including standard error. All images were collected in a 512x512 pixel format with a 63x 1.4 NA oil objective.

Computer analysis

Analysis of *Streptomyces* genes and proteins was done at the StrepDB database (http://strepdb.streptomyces.org.uk/). For phylogenetic analysis and correlations the String engine (http://string.embl.de) was used, while putative transmembrane domains were identified using transmembrane prediction server DAS (http://www.sbc.su.se/~miklos/DAS/).

RESULTS

SsgB shows exceptional evolutionary conservation, whereby a maximum of one amino acid (aa) change is seen in orthologs from the same genus, while conversely, conservation is low between different actinomycete genera, even if they are closely related (Girard et al., 2013). During recruitment of FtsZ, SsgB docks to the membrane, but the lack of a predicted membrane domain suggests that another protein ensures its membrane attachment. To search for candidate membrane docking proteins, an *in silico* analysis of the estimated 1850 membrane proteins of *S. coelicolor* was performed. Considering the peculiar conservation of SsgB, we narrowed down the number by searching for proteins with >90% aa identity between the *Streptomyces* orthologs, and lower conservation (<70% aa identity) between orthologs in other actinomycete genera. The 20 best hits are listed in Table 4. Of these, *ylmG* (SCO2078) stood out. Its genomic location in-between *sepF* (controls the polymerization of FtsZ) and *divIVA* (controls the septum site in *B. subtilis*) suggests a role in the earliest phase of cell division. Furthermore, the predicted cytoplasmic domain consisting of aa residues 30-69 shows a very similar conservation as SsgB, with near complete conservation between the *Streptomyces* orthologs (99-100%), but low conservation (50-60% aa identity) between *Streptomyces* and other actinomycetes. Interestingly, the TM domain is less well conserved, consisting with possible covariation of especially the YlmG cytoplasmic domain and SsgB.

The *ylmG* gene encodes a 95 aa protein and lies upstream of *divIVA* (SCO2077) and downstream *sepF* (SCO2079) in the *dcw* cluster of *S. coelicolor*, whereby *sepF* and *ylmG* are likely cotranscribed. YlmG has an N-terminal and a C-terminal transmembrane domain, with the central part of the protein predicted to reside intracellularly. The distribution of *ylmG* includes the phylum of the Actinobacteria (high G+C Gram positives), which encompasses both sporulating and nonsporulating genera, several Firmicutes (low G+C Gram positives), including *Bacillus* and *Streptococcus*, as well as Cyanobacteria and chloroplasts. A detailed phylogenetic tree was presented by Kabeya and colleagues (Kabeya *et al.*, 2010). The wide distribution of YlmG suggests an ancient common ancestor.

Table 4. Membrane proteins with high conservation in streptomycetes but lower conservation between different actinomycete genera. The 20 best hits are listed.

SCO #	Protein	Function	Conservation ^
SCO1541	SsgB [a]	Cell division protein	99
SCO4609	HtpX	Metallopeptidase	97
SCO2155	Cox1	Cytochrome C oxidase subunit I	96
SCO2151	Cox3	Cytochrome C oxidase subunit III	96
SCO2078	YlmG	Membrane protein	96
SCO2944		Sugar permease subunit	95
SCO4602	NuoH2	NADH dehydrogenase subunit	95
SCO1389	ClsA	Cardiolipin synthase	95
SCO5118	OppB	oligopeptide permease subunit	95
SCO3404	FtsH2 [b]	metalloprotease	95
SCO1527		Alcohol phosphatidyl transferase	94
SCO2534		hemolysin-like protein	93
SCO1796		Stomatin-like protein	93
SCO2150	QcrC	Cytochrome C heme-binding subunit	93
SCO5670		putative polyamine permease subunit	93
SCO2945		Sugar permease subunit	93
SCO2148	QcrB	Cytochrome B subunit	93
SCO4722	SecY	Preprotein translocase subunit	92
SCO1215	CtaG	Cytochrome c oxidase assembly factor	92
SCO3945	CydA	Cytochrome ubiquinol oxidase subunit	92
SCO2087	MurX	phospho-N-acetylmuramoyl-pentapeptide-transferase	92

according to the *Streptomyces coelicolor* database numbering.

^ average aa identity (in %) between streptomycetes. For this comparison the eight genomes of the streptomycetes in StrepDB were used. The value is on average 2-3% lower if *S. lividans* is not included.

[a] included for reference purposes.

[b] does not occur in all streptomycetes.

ylmG null mutants are defective in sporulation

To study the function of *ylmG* in *Streptomyces*, an in-frame deletion mutant was created in *S. coelicolor* M145. For this, gene replacement construct pGWS731 (see Materials and Methods section) was introduced into *S. coelicolor* M145 and colonies selected for apramycin resistance (marker for *ylmG* disruption) and sensitivity to thiostrepton (marker for the vector). These colonies presumably had *ylmG* replaced by the apramycin resistance cassette on the genome. Expression of the Cre recombinase in these cells resulted in a number of markerless deletion mutants, which all had very similar pheno-

types with impaired sporulation as judged by the lack of grey pigmentation. After PCR verification of the deletion of *ylmG* in these colonies, one representative colony was then selected and designated GAL1.

Growth on SFM agar plates showed that *ylmG* mutants were impaired in development. While the parental strain *S. coelicolor* M145 developed normal grey-pigmented colonies indicative of sporulation, the *ylmG* null mutant GAL1 had a nearly white phenotype, eventually showing light-grey pigmentation (Fig. 1A). The sporulation defect was confirmed by phase-contrast light microscopy of impression prints of surface-grown colonies, which demonstrated that GAL1 produced only very few spore chains (Fig. 1B). Introduction of plasmid pGWS771, which is a low-copy number vectors expressing *ylmG* behind the *ftsZ* promoter (see below), restored sporulation to the mutant, indicating that the sporulation deficiency was indeed due to the deletion of *ylmG*.

Closer inspection of the aerial hyphae and spores by cryo-scanning electron microscopy (SEM) showed that where the parental strain *S. coelicolor* M145 produced abundant spiraling hyphae and well-developed chains of spores, the *ylmG* null mutant predominantly produced straight aerial hyphae, whereby only very few chains of irregularly shaped spores could be identified (Fig. 2A). To quantify the size distribution, approximately 130 spores from the *ylmG* mutant and the wild-type strain *S. coelicolor* M145 were measured. While wild-type spores showed the typical Gaussian distribution centered around 0.8-1.2 μm in length, *ylmG* mutant spores showed a broader distribution, with an average size (1.3 μm) of around 0.2 μm larger than wild-type spores (1.1 μm). These data identify *ylmG* as a novel sporulation gene involved in sporulation-specific cell division and the gene was therefore renamed *sepG*.

1A

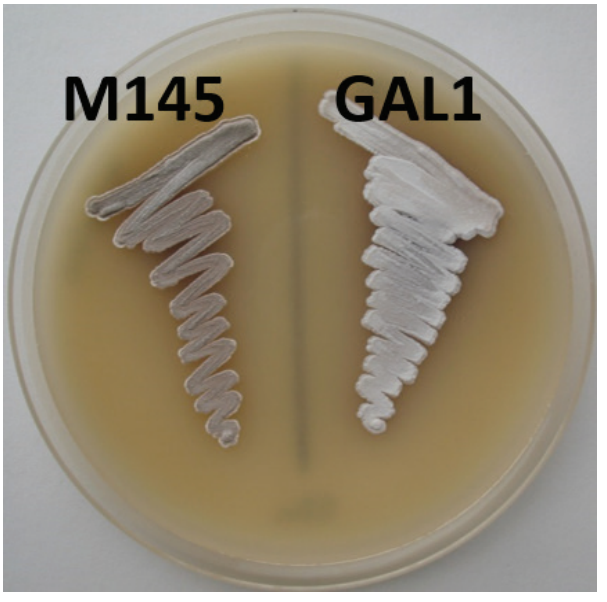

1B

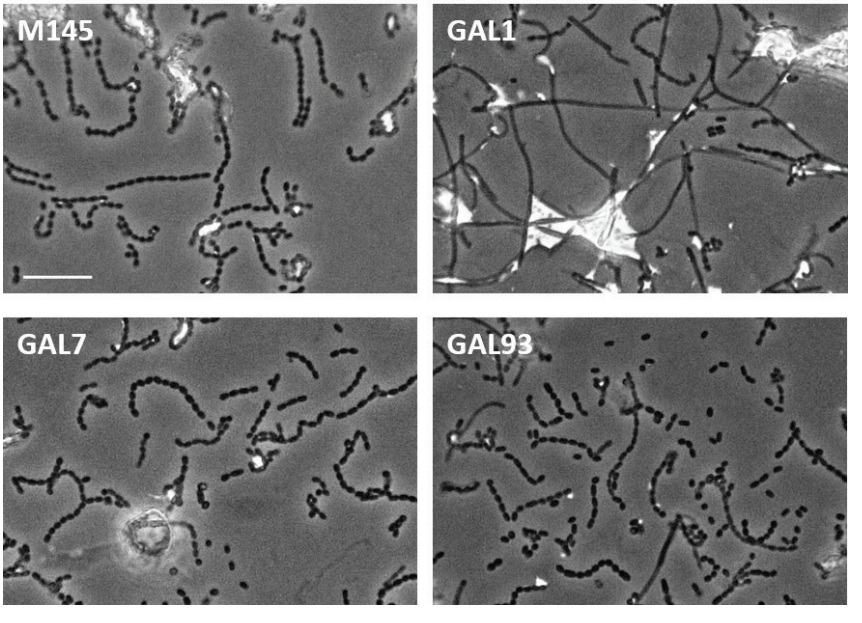

Figure 1. Light micrographs of the *ylmG* null mutant of *S. coelicolor*. **(A)** Comparison of *S. coelicolor* M145 and its *ylmG* null mutant GAL1. Note the lack of grey pigmentation of the *ylmG* mutant due to failure to produce the grey spore pigment. **(B)** Phase-contrast light micrographs of impression prints from cultures grown on SFM agar. Note that expression of wild-type YlmG (GAL93) or YlmG-eGFP (GAL7) restores sporulation to the *ylmG* mutant. All cultures were grown on SFM agar plates for 5 days at 30^0C. Bar, 10 μm.

2A

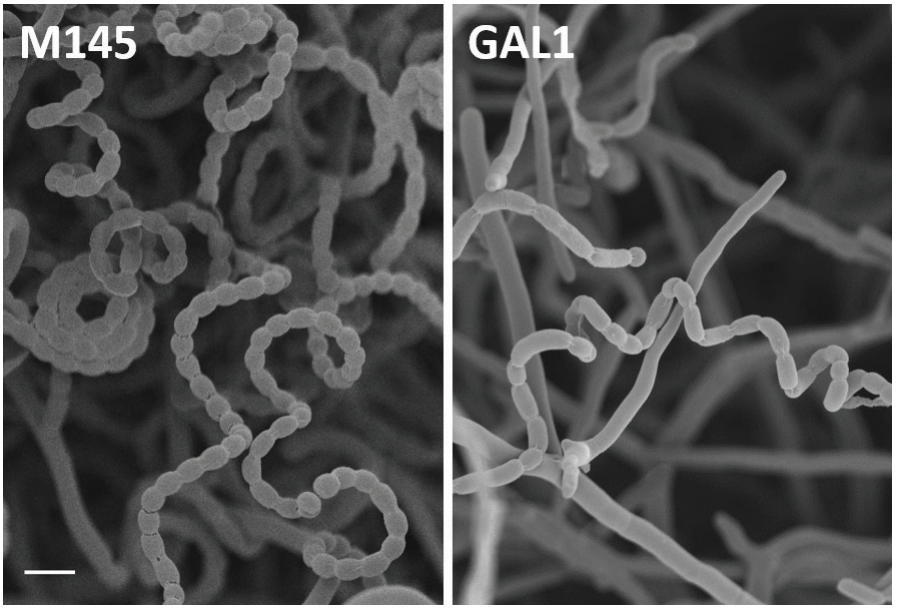

2B

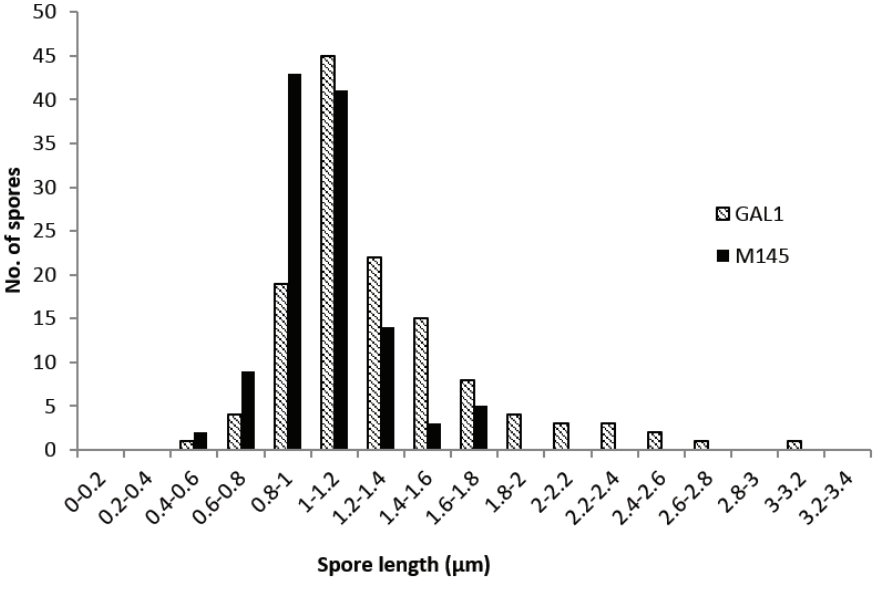

Figure 2. Comparison of spores produced by wild-type *S. coelicolor* M145 and its *ylmG* null mutant. (A) Cryo-scanning electron micrographs of wild-type and *ylmG* mutant aerial hyphae. Wild-type sporulated abundantly, while occasional chains of irregularly sized spores were produced by the *ylmG* mutant. Cultures were grown on SFM agar plates for 5 days at 30^{0}C. Bar, 2 µm. **(B)** Size distribution of wild-type and *ylmG* mutant spores. Spores were measured from a representative number of cryo-scanning electron micrographs, so that around 130 spores were measured for each strain. Note that a significant number of *ylmG* mutant spores were unusually long.

SepG is required for proper spore-wall synthesis and nucleoid morphology

To obtain more detailed insight into spore morphology and spore-wall thickness, we performed high-resolution imaging using transmission electron microscopy (TEM) on thin sections. This again revealed the irregular sporulation of the *sepG* mutant. Furthermore, *sepG* mutant spores contained a considerably thinner and more electron-lucent cell wall, indicative of altered spore-wall synthesis (Fig. 3). Another major alteration observed in *sepG* mutant spores was the shape of the spore nucleoid. Rather than a well-condensed nucleoid in the center of the spores as seen in wild-type spores, the *sepG* mutant spores show a less well condensed nucleoid that primarily localized close to the edge of the spores, with a pattern suggesting an unusual toroidal or doughnut shape (Fig. 3). Notably, such a doughnut shape is found routinely for nucleoids in developing or germinating spores of *Bacillus*.

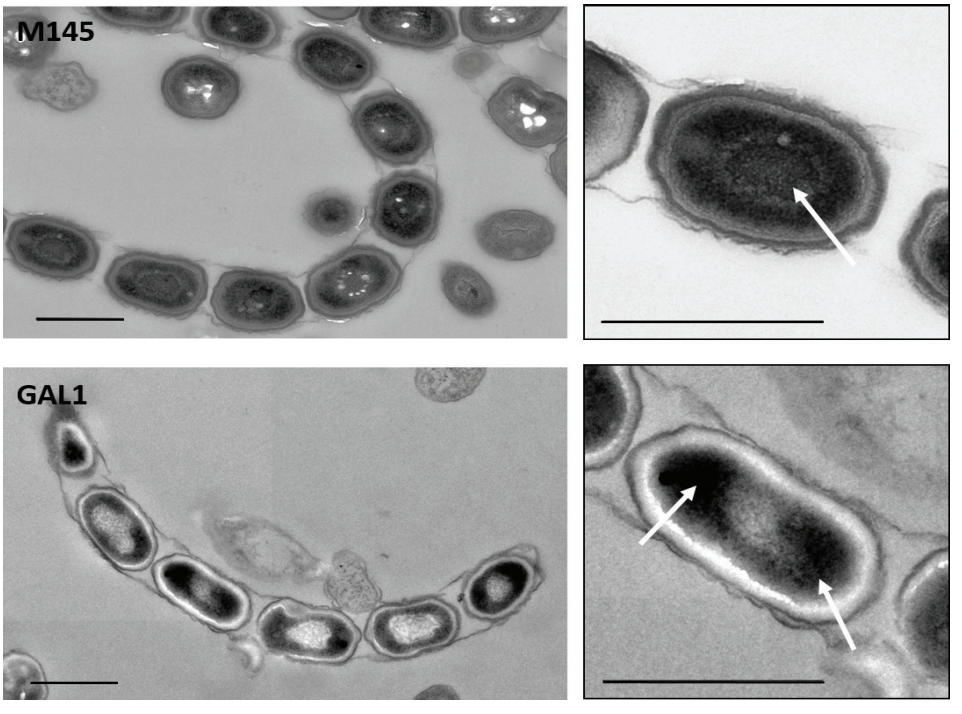

Figure 3. Transmission electron micrographs of wild-type and *sepG* mutant spores. Both a representative overview (left) and close-up (right) are presented. Arrows indicate nucleoids. Note that whereas the wild-type (M145) nucleoid is well condensed and located at the center of the spores, that of the *sepG* mutant (GAL1) has an unusual distribution. Note the lighter appearance of the spore wall in the *sepG* mutant. Cultures were grown on SFM agar plates for 5 days at 30^0C. Bar, 1 µm.

Viability of the *sepG* mutant spores was tested by analyzing heat resistance. For this, spores were incubated for 10 minutes at 60°C and plated onto SFM agar plates. While 45% of the wild-type spores survived the heat treatment, survival of the *sepG* mutant spores was as low as 8%. The defect could be largely complemented by expressing SepG: 36% and 32% of spores of GAL93 and GAL7 survived the heat treatment, repectively. GAL93 is the *sepG* mutant transformed with pGWS771, which harbors wild-type *sepG*. GAL7 is the *sepG* mutant harboring localization construct pGWS755.

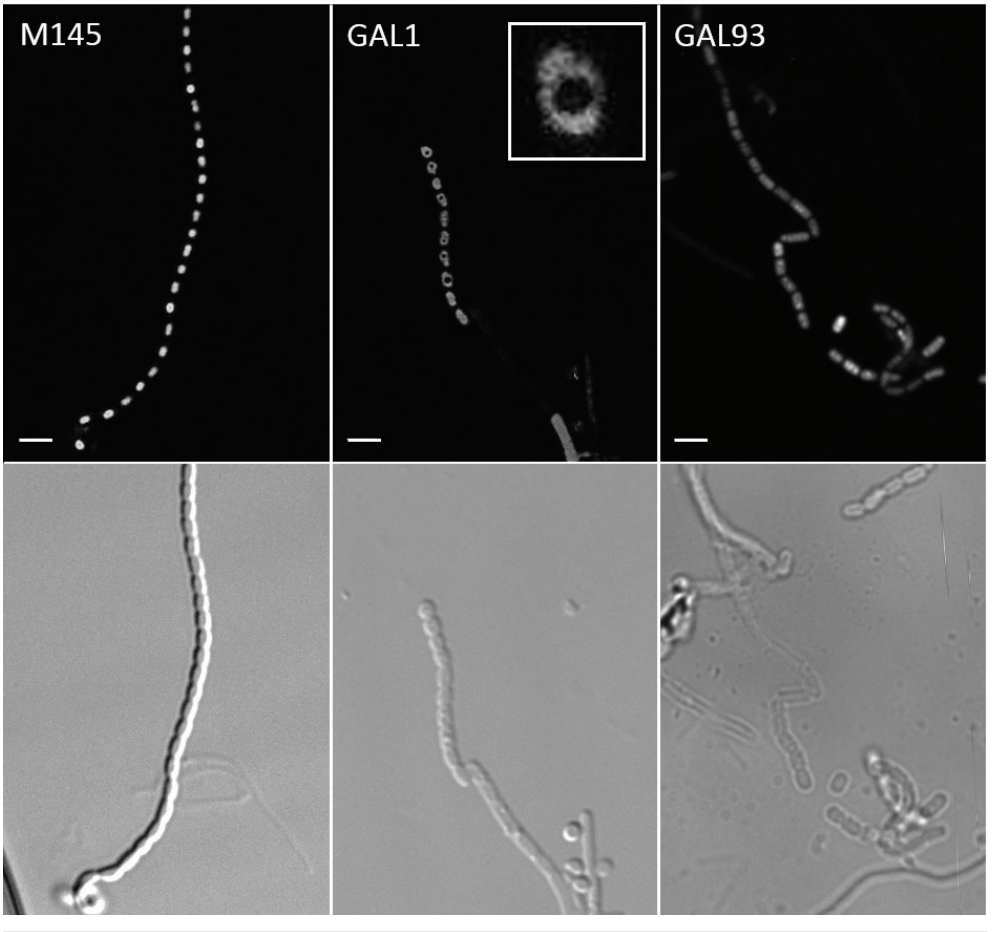

Figure 4. Fluorescence micrographs of nucleoid distribution in the spores by STED. Top, STED images; bottom, light images. DNA staining of wild-type spores (M145, left) shows normal spore lengths and proper nucleoid condensation. In contrast, nucleoids of *sepG* null mutants (GAL1, middle) appear doughnut shaped and less well condensed. The aberrant nucleoid shape is complemented by a clone expressing *sepG* (transformant GAL93, right), but DNA condensation is still affected. Inset: 7x magnification of one of the nucleoids. Cultures were grown on SFM agar plates for 5 days at 30^0C. Bar, 2 μm.

To visualize the nucleoid distribution in wild-type and *sepG* mutant spores, the nucleoids were stained with Syto 9 and imaged with stimulated emission depletion (STED) microscopy (Fig. 4). In wild-type spores, the nucleoids were seen as very bright dots that localized to the central part of the spores. Interestingly, in *sepG* null mutants the nucleoids were less condensed and more dispersed, whereby the centers of the spores were largely devoid of DNA. Spores of strain GAL93, which is the *sepG* null mutant containing plasmid pGWS771 expressing wild-type *sepG*, no longer showed such doughnut-shaped DNA structures, although the nucleoids appeared less well-condensed as compared to wild-type spores. Thus, TEM and STED data suggest that SepG is required for proper nucleoid compaction during sporulation.

Localization of SepG

To determine the localization of SepG in *S. coelicolor*, a C-terminal fusion with enhanced green fluorescent protein (eGFP) was constructed under the control of the *ftsZ* promoter (plasmid pGWS755). Introduction of pGWS755 into the *sepG* null mutant restored sporulation and spore viability, which shows that SepG-eGFP is functional *in vivo*. Confocal fluorescence microscopy was applied to investigate SepG-eGFP localization in wild type cells and the *sepG* mutant. The pattern of SepG-eGFP localization was dynamic and developmental stage-dependent. In young aerial hyphae, when the chromosomal DNA was still uncondensed and septal membrane synthesis had not yet initiated, SepG-eGFP formed distinct and widely spaced foci (Fig. 5A). Importantly, such a localization pattern is very similar to that of the initial stage of SsgB localization, prior to its septum-site localization ((Willemse *et al.*, 2011) and Fig. 6). During the subsequent spore maturation the nucleoids condensed, and at this stage SepG-eGFP relocalized to the intersection between the spores, which at this point in spore development is the only place where active cell-wall remodeling takes place (Fig. 5B). In the merged images, SepG-eGFP localized to the nucleoid-free zones in spores, with a ring of SepG surrounding the nucleoid (Fig. 5C). The fluorescence images strongly suggest that in *sepG* mutant spores, the nucleoid takes up the space normally occluded by a SepG-dependent mechanism, and it suggests that SepG and DNA may be mutually exclusive (Fig. 5D). In mature spores, which are physically separated, no GFP signal could be observed, suggesting that SepG eventually disappears (not illustrated).

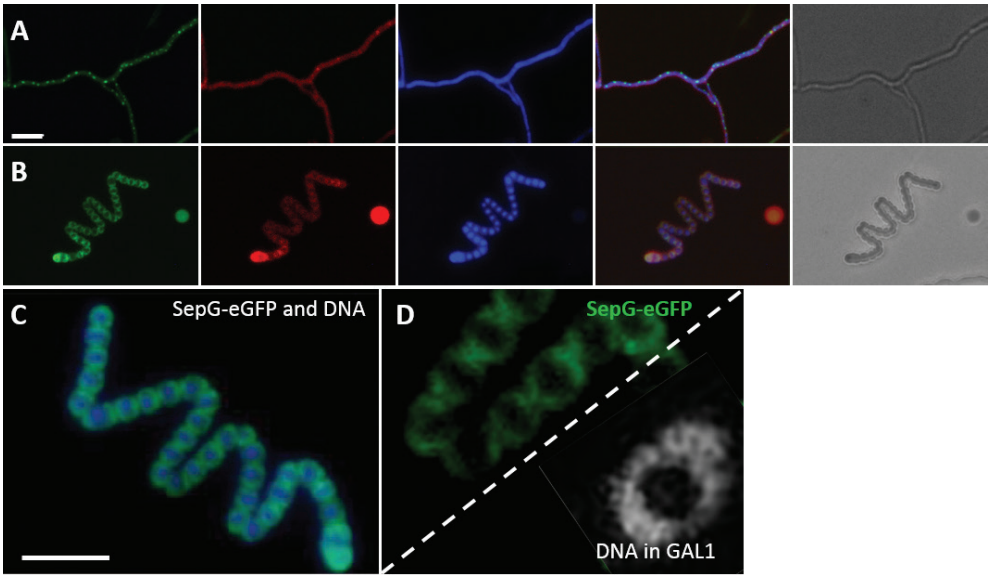

Figure 5. Localization of SepG-eGFP. Sporogenic aerial hyphae of *S. coelicolor* M145 were imaged by Fluorescence microscopy visualizing SepG-eGFP, membrane (stained with FM5-95), DNA (DAPI), the merged image and a light micrograph at the onset of sporulation in aerial hyphae **(A)** and during sporulation **(B)**. **C** represents a merged image of SepG-eGFP and the DNA taken from (B). Image **D** shows that SepG-eGFP in wild-type cells (left) has a similar localization in the spores as the DNA in the *sepG* null mutant (right), which suggests a model whereby SepG acts to condense the DNA in the center of the spores. Bar, 5 μm.

Localization of SsgB to septum sites depends on direct interaction with SepG

We previously showed that FtsZ is directly recruited by SsgB in an SsgA-dependent manner, followed by recruitment of the other divisome components (Willemse *et al.*, 2011). The phenotype of the *sepG* null mutants prompted us to investigate whether the localization of one or more of these proteins was affected by the absence of SepG. To address this question, pGWS116, pGWS526 or pKF41, expressing SsgA-eGFP, SsgB-eGFP or FtsZ-eGFP, respectively, were introduced into the *sepG* null mutant. While SsgA-eGFP localized normally in the mutant, SsgB-eGFP was mainly seen to localize diffusely along the hyphal membrane, instead of the focal pattern at future septum sites seen in sporogenic aerial hyphae of the parental strain M145. This is consistent with a model where SepG is required for the membrane docking of SsgB after its initial localization by SsgA (Fig. 6A). In line with the delocalized pattern of the FtsZ-recruiting SsgB protein, the *sepG* mutant also failed to produce the

typical ladder patterns of FtsZ-eGFP seen in wild-type hyphae (Fig. 6A). Only occasional septa were formed, a phenotype that is also observed in *ssgB* null mutants and other sporulation (*whi*) mutants (Willemse *et al.*, 2011). Interestingly, SsgB-eGFP still formed distinct foci in the middle of the hyphae, with around 1 μm spacing, typical of the first stage of SsgB localization (Fig. 6B). However, in contrast to SsgB in wild-type cells (Willemse *et al.*, 2011), in the *sepG* null mutant the foci subsequently disappeared, indicating that the stable localization of SsgB requires SepG. Thus, after SsgA ensures the initial localization of SsgB, SepG then acts to ensure the membrane association of SsgB at division sites, which is the first step in sporulation-specific cell division.

6A

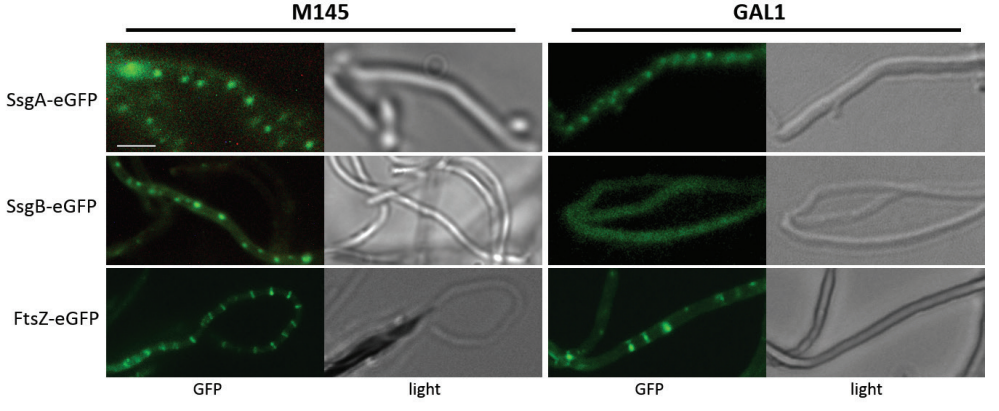

6B

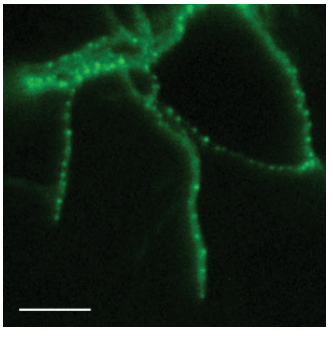

Figure 6. Effect of SepG on the localization of eGFP fusions of SsgA, SsgB and FtsZ. (A) all proteins localize correctly in wild-type cells (M145, left). In contrast, SepG is required for the formation of ladders of FtsZ or for the localization of SsgB at division sites. SsgA has a normal focal pattern in the *sepG* mutant. The occasional Z rings formed by *sepG* mutants are also seen in *ssgB* mutants of *S. coelicolor* (see the text for references). Bar, 2 μm. **(B)** SsgB temporarily forms foci in the central part of the aerial hyphae, but fails to localize to the membrane. Cultures were grown on SFM agar plates for 5 days at 30^0C. Bar, 5 μm.

This raised the question whether the mislocalization of SsgB and FtsZ could be explained by direct interaction between SepG and SsgB. To investigate this *in vivo*, we applied Förster resonance energy transfer (FRET), which allows the identification of direct molecular interactions. As low-wavelength fluorophore eGFP was used, and as longer-wavelength fluorophore mCherry. YlmG-mCherry was introduced into *S. coelicolor* M145 expressing either SsgA-eGFP or SsgB-eGFP to generate strains GAL94 and GAL95, respectively; YlmG-eGFP was introduced into *S. coelicolor* M145 expressing FtsZ-mCherry to generate strain GAL96. Strains JSC2 and JSC3, which are *S. coelicolor* FM145 co-expressing SsgB-eGFP with FtsZ-mCherry, and SsgB-mCherry with FtsZ-eGFP, respectively, were used as positive controls, based on the direct interaction between SsgB and FtsZ (Willemse *et al.*, 2011). As negative control we used *S. coelicolor* K202, which expresses FtsZ-eGFP alone.

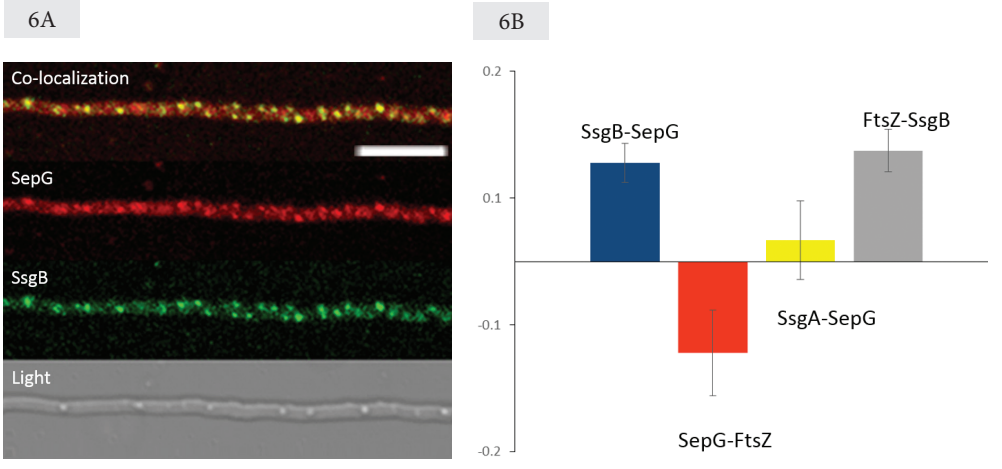

Figure 7. FRET imaging of the interaction between SepG and SsgB. (A) FM images showing the colocalization of SsgB and SepG. Bar, 5 μm. **(B)** Graphical representation of the FRET data. All efficiencies are represented relative to the control (which was set to zero). FRET data are summarized in Table 5.

Table 5. FRET efficiencies for different combinations of donor (eGFP) and acceptor (mCherry).

Strain	GAL95	GAL96	GAL94	JSC3	JSC2
Donor-acceptor	SsgB-SepG	SepG-FtsZ	SsgA-SepG	FtsZ-SsgB	SsgB-FtsZ[#]
Average FRET Efficiency	1.05	0.90	0.99	1.06	1.25
Standard deviation	0.02	0.03	0.03	0.02	0.21

[#] not included in Fig. 7B to allow better comparison.

JSC2 and JSC3 showed a FRET efficiency consistent with the short intermolecular distance between FtsZ and SsgB (Table 5). The molecular ratio between SsgB and FtsZ (approximately 1:3) explains why JSC2 yields a higher FRET efficiency as compared to JSC3, as the energy of one SsgB-eGFP can be transferred to multiple FtsZ-mCherry molecules while the energy of multiple FtsZ-eGFP molecules can only be transferred to one molecule of SsgB-mCherry. The negative control FtsZ-eGFP had a FRET efficiency of 0.97 ± 0.02, consistent with lack of interaction with an acceptor (Table 5). Interestingly, SepG and SsgB colocalized very well, with over 90% overlap of the foci (Fig. 7A). The two proteins also closely interact, as shown by the FRET efficiency of 1.05 ± 0.02 which suggests an intermolecular distance that is close to that between the known partners SsgB and FtsZ. No interaction was seen for SepG and SsgA (FRET efficiency of 0.99 ± 0.03) or SepG and FtsZ (0.90 ± 0.03). The data are summarized graphically in Fig. 7B, whereby the negative control was set to zero. These FRET data are consistent with direct interaction between SepG and SsgB *in vivo*, while no interaction was seen between SepG and either SsgA or FtsZ. Taken together, our data suggest that SepG and SsgB directly interact, whereby SepG is required for the septal localization of SsgB, which in turn recruits FtsZ to division sites to initiate sporulation-specific cell division in *S. coelicolor*. After cell division commences, SsgB remains on the divisome while SepG follows sites of active cell-wall remodeling, where it coordinates nucleoid compaction to keep the DNA away from the cell wall.

DISCUSSION

The control of cell division in the multicellular streptomycetes is very different from that in for example *E. coli* and *B. subtilis* (Claessen *et al.*, 2014). During sporulation, the aerial hyphae differentiate into long chains of spores, and the more or less simultaneous formation of many septa results in spectacular ladders of Z rings (Schwedock *et al.*, 1997). The canonical control systems and septum-localizing proteins (Min, Noc, FtsA, ZipA, ZapA, EzrA, etc.) found in bacteria that divide by binary fission are all absent in streptomycetes, and instead actinomycete-specific proteins control the localization of the septa. In streptomycetes cell division is positively controlled, whereby FtsZ is actively recruited to septum sites by the action of SsgB (Willemse *et al.*, 2011). SsgB is a member of the family of SsgA-like proteins, which exclusively occur in actinomycetes. While the role of SsgB explains how FtsZ is localized to the future septum sites, and the SsgA protein plays an active role in its localization (Willemse *et al.*, 2011), how the striking symmetry of the Z ladders is controlled, has so far remained unresolved.

In this work, we show that *ylmG,* which lies in-between *sepF* and *divIVA*, and is one of the last genes in the *dcw* cluster whose function had not yet been established, plays a major role in the control of sporulation-specific cell division in *S. coelicolor*. The gene was therefore renamed *sepG*. In streptomycetes, SepG apparently has two roles during sporulation-specific cell division. Firstly, SepG helps to orchestrate the earliest stage of sporulation-specific cell division, as it directly binds to SsgB and likely acts as a membrane anchor to ensure the localization of SsgB to future septum sites. After the initial localization of SsgB by SsgA to a central position in the aerial hyphae, this is the next crucial step in the positive control of cell division in *Streptomyces*, followed by the recruitment of FtsZ by SsgB. Secondly, at a later stage of spore development, SepG is required for synthesis of the mature spore wall as well as for maintaining nucleoid shape. In wild-type cells, SepG forms a ring that surrounds the nucleoid, while in *sepG* null mutants large doughnut-shaped nucleoids are formed accompanied by less dense spore wall, suggesting imperfect cell wall synthesis; the latter is consistent with the lower heat sensitivity of the spores. Taken together, these data suggest that during early sporulation, SepG allows SsgB to find the future sites of division, where after SepG continues to follow the spore-wall synthetic machinery, and ensures the coordination of spore-wall synthesis with nucleoid compaction by a mechanism that is yet unresolved.

FRET data revealed direct interaction between SepG and the FtsZ-recruit-

ing SsgB. Interestingly, the cytoplasmic domain of SepG shows a similar conservation as SsgB, with extremely high conservation in streptomycetes, but low conservation between different actinomycete genera. Such a conservation pattern is not evident in the transmembrane domains. The suggestive covariation in terms of aa conservation in different bacteria between the SepG cytoplasmic domain and SsgB provides supporting phylogenetic evidence consistent with direct interaction between SsgB and SepG. Furthermore, SsgB fails to localize specifically to the septum site in *sepG* null mutants, which also explains the mislocalization of FtsZ. The early co-localization of and direct interaction between SepG and SsgB implies that either SepG ensures the correct localization of SsgB, or *vice versa*. The fact that SepG localizes normally in *ssgB* mutants, while conversely, SsgB does not localize properly in *sepG* mutants, supports the former model. Interestingly, time-lapse imaging showed that in the absence of SepG, SsgB temporarily localizes to a central position in the hyphae, very similar to SsgA, but then rapidly disperses along the membrane rather than finding the future division sites. This strongly suggests a model whereby SsgA recruits SsgB to a central position in the hyphae, followed by the subsequent SepG-dependent docking of SsgB to the future division sites. It also suggests that SsgB has affinity for the membrane, which may be explained by the large hydrophobic patch in the SsgB trimeric structure (Xu *et al.*, 2009). SsgB then actively recruits FtsZ and assists in its polymerization, whereby SsgB remains part of the divisome and follows FtsZ throughout the process of cell division (forming the same ladders as FtsZ).

The joint movement of SepG and SsgB to the division sites also ensures that SepG arrives at the first site of peptidoglycan synthesis during sporulation, which is the septum. From there, the membrane protein SepG follows the spore-wall synthetic machinery, somehow ensuring that the DNA is kept away from this construction site and preventing lethal damage. It is yet unclear how SepG controls the nucleoid shape in *Streptomyces*. While relatively little is known of nucleoid dynamics in *Streptomyces*, we can try to glean information from the well-studied *B. subtilis*, although *Bacillus sepG* null mutants have no apparent phenotype (Hamoen et al., 2006). While during vegetative growth the nucleoid localizes close to mid-cell in *B. subtilis*, its shape changes during the onset of sporulation, and eventually a doughnut-shaped ring is formed similar to that found in *S. coelicolor sepG* mutants, with a diameter of around 1 μm (Pogliano *et al.*, 1995). During germination, these rings disappear and the nucleoids take up the diffuse lobular shape typical of vegetative cells (Ragkousi *et al.*, 2000). The nucleoid ring in *Bacillus* spores is maintained by the action of small acid soluble proteins (SASPs), encoded by the *sspA* genes. SASPs, which

are absent from streptomycetes, change the conformation of the DNA from B to A (Mohr et al., 1991) and also protect spores against heat, UV damage or oxidative stress (Mason and Setlow, 1987). Deletion of *sspA* genes results in collapse of the nucleoids towards the center of the spores (Setlow et al., 2000). In other words, the opposite occurs as compared to *Streptomyces*, where the wild-type nucleoid is condensed in the center of the spores, while deletion of *sepG* results in ring formation.

The expansion of the nucleoid towards the membrane likely contributes to disturbance of the cell cycle, as this is expected to trigger a nucleoid-occlusion like mechanism to prevent septum synthesis close to the nucleoid, even though such a mechanism has not yet been identified in streptomycetes. This includes various mutants disturbed in DNA partitioning, such as *parA* and *parB* mutants of *S. coelicolor*. We previously showed that the SsgA-like protein SsgC plays a role in nucleoid segregation, with highly disturbed distribution of DNA in *ssgC* null mutants (Noens et al., 2005). It is tempting to suggest that other SALPs may also interact with SepG, with SsgC as one of the candidates.

Since SsgB only occurs in actinomycetes, one may wonder how universal the function of SepG is. We expect that the principles shown in this work will translate to lower Gram-positives such as *Bacillus* and *Streptococcus*, which is among others based on strong phylogenetic evidence, since the location of *sepG* between *divIVA* and *sepF* was maintained during several hundred millions years of evolution, although *ylmH* was lost in actinomycetes. Therefore, functional overlap between the *Bacillus* and *Streptomyces* orthologs is to be expected. In this light, a key observation may well be that like in *Streptomyces*, a cell division control mechanism that is independent of the negative control systems Min and Noc has recently been identified in *B. subtilis*. It was shown that the Z ring can be positioned at division sites in the absence of Min and Noc, and that in Noc$^-$ cells the Z rings have a preference for the mid-cell position between the two nucleoids (Rodrigues and Harry 2012). Conceivably therefore, SepG may have a similar role in division-site selection in *B. subtilis* as in *Streptomyces*, but such a role would only be obvious if *sepG* were to be studied – and, if at all possible, mutated - in the absence of Noc. Further molecular insights into the function of SepG in streptomycetes will shed more light on the way the positive control of cell division is governed in these multicellular bacteria, as well as on the yet poorly understood mechanisms that prevent nucleoid damage during septum synthesis and cell-wall remodeling.

Acknowledgements

We are very grateful to Leendert Hamoen for discussions and for comments on the manuscript. The work was supported by ECHO and VICI grants from the Netherlands Organization for Scientific Research (NWO) to GPvW.